ELSEVIER

Catalysis Today 71 (2001) 199–210

CATALYSIS TODAY

www.elsevier.com/locate/cattod

The direct partial oxidation of methane to organic oxygenates using a dielectric barrier discharge reactor as a catalytic reactor analog

David W. Larkin*, Lance L. Lobban, Richard G. Mallinson

Institute for Gas Utilization Technologies and School of Chemical Engineering and Materials Science, University of Oklahoma, 100 E. Boyd, Rm T 335, Norman, OK 73019, USA

Abstract

The present work discusses the direct oxidative conversion of methane to organic oxygenates (methanol, formaldehyde, methyl formate, and formic acid) using a dielectric barrier discharge (DBD) reactor. The DBD reactor can be considered an analog to a catalytic reactor because, just as with the catalytic reactor, the DBD reactor reduces the required temperature and pressure needed for reactions to occur within it as well as control product selectivity. In this study, the effects of changing the electrical properties within a methane–oxygen DBD system were investigated. Increasing the gas gap from 4.0 to 12.0 mm caused the reduced electric field to decrease from 30 to 18 V/cm/Torr, which resulted in a shift in the product distribution from organic oxygenate liquids to ethane and acetylene. The effects of temperature on product selectivity were also studied through the use of a water jacket. Lowering the temperature of water within the water jacket from 75 to 28°C resulted in a 54% increase in organic oxygenate selectivity and a 56% decrease in CO_x selectivity.

Keywords: Methane; Methanol; Dielectric barrier discharge; Reduced electric field; Atomic oxygen

1. Introduction

Natural gas is looked upon as a desirable fuel, since it is clean burning with vast reserves worldwide. Many of the these reserves, however, are located in remote areas and, therefore, it is economically infeasible to transport the gas via pipeline. One alternative is to convert the natural gas into an organic liquid, such as methanol, at the production site which would greatly reduce the transportation cost. The current commercial methanol synthesis technology is an energy intensive two-step process in which the first step is methane-steam reforming. In this first step, shown below, a nickel base catalyst is used with an operating temperature range 500–1100°C and an operating pressure range 15–30 atm [1,2].

$$CH_4 + H_2O \leftrightarrow 3H_2 + CO,$$
$$\Delta H_{298\,K} = 206\,kJ/mol \quad \text{(reaction 1)}$$

$$CO + H_2O \leftrightarrow CO_2 + H_2,$$
$$\Delta H_{298\,K} = -41\,kJ/mol \quad \text{(reaction 2)}$$

The methane-steam reforming reaction (reaction 1), which is endothermic, is thermodynamically favored by high temperature and low pressure. On the other hand, the water–gas shift reaction (reaction 2) is not pressure dependent and is favored by low temperature (exothermic reaction). However, heat produced by the second reaction is never able to make up for the heat required for the first reaction and the overall reaction is endothermic

$$CH_4 + 2H_2O \leftrightarrow CO_2 + 4H_2O,$$
$$\Delta H_{298\,K} = 165\,kJ/mol \quad \text{(reaction 3)}$$

* Corresponding author.

0920-5861/01/$ – see front matter
PII: S0920-5861(01)00430-8

Thus, furnaces are required for additional heat input. Two-thirds of the operating costs of the overall process come from this first step [1–3]. This product stream is then fed to the methanol synthesis stage (second step). The catalyst used in this step is a $Cu/ZnO/Al_2O_3$ catalyst (operating temperature range is 220–300°C and the operating pressure range is 50–100 atm). The two important reactions that occur within this stage, shown below, are exothermic [1,2]:

$$CO + H_2O \leftrightarrow H_2 + CO_2,$$
$$\Delta H_{298\,K} = -41.2\,kJ/mol,$$
$$\Delta G_{298\,K} = -28.6\,kJ/mol \quad \text{(reaction 4)}$$

$$CO_2 + 3H_2 \leftrightarrow CH_3OH + H_2O,$$
$$\Delta H_{298\,K} = -49.5\,kJ/mol,$$
$$\Delta G_{298\,K} = -3.3\,kJ/mol \quad \text{(reaction 5)}$$

The overall reaction, in which for every 3 mol of feed converted (1 mol CO+2 mol of H_2), 1 mol of methanol is formed, is exothermic

$$CO + 2H_2 \leftrightarrow CH_3OH, \quad \Delta H_{298\,K} = -90.6\,kJ/mol,$$
$$\Delta G_{298\,K} = -25.3\,kJ/mol \quad \text{(reaction 6)}$$

Due to the fact that the commercial methanol synthesis process is energy intensive, it may not be economical when the natural gas is in remote places or expensive. However, a desirable alternative maybe the direct partial oxidation of methane to methanol since a one-step process could potentially reduce both capital and operating costs. Currently, there is no economical one-step direct partial oxidation of methane to methanol process; however, a non-equilibrium plasma reactor (dielectric barrier discharge (DBD) reactor) might be a possible solution. Non-equilibrium plasmas are plasmas in which the electron kinetic energies are much higher than those of neutral species [4].

Further, a DBD reactor (non-equilibrium plasma reactor) can be considered an analog to a catalytic reactor. This is because both reactors reduce the pressure and temperature needed for reactions to occur within them. In the case of catalytic reactor, this is done by the catalyst lowering the activation energy required for a reaction to occur. On the other hand, the DBD reactor is able to do this by using high energy electrons to initiate reactions. Thus for the DBD reactor, the operating temperature and pressure within the reaction zone can be quite low (e.g., room temperature and atmospheric pressure).

In addition, both catalytic and non-equilibrium plasma reactor systems are used to control the product selectivity. An example for controlling selectivity in a catalytic system is shown in the second step of the commercial methanol synthesis process, in which undesirable side reactions to hydrocarbons, ethers, and higher alcohols are thermodynamically more favored than the formation of methanol. Therefore, the 99.9% selectivity for methanol obtained in the commercial process is due to the fact that methanol selectivity is controlled by the catalyst favoring the methanol pathway [1,2].

In the case of the DBD reactor, the selectivity is controlled by the electron energy distribution within the system. The electron energy distribution in a DBD reactor can be altered by changing various system parameters (e.g., gas gap and system pressure). This in turn affects the energy deposition directed toward the various electron–gas species collision processes. Hence, the chemistry occurring within the reaction zone is controlled by changing the electrical properties of a gas-phase system within the DBD reactor.

These electrical properties can be characterized through Bolsig, an electron Boltzmann equation by Kinema Software and CPAT [6]. This electron Boltzmann solver is designed for systems that have steady-state, uniform electric fields (E) with weakly ionized gases, which is the case for a DBD system [6]. This program numerically solves for the Boltzmann equation, shown below, which describes the electron energy distribution function (f) in terms of space (x), velocity (v), and time (t) [4–6]:

$$\frac{\partial}{\partial t} f(x, v, t) + a \frac{\partial}{\partial v} f(x, v, t) + v \frac{\partial}{\partial x} f(x, v, t) = \frac{\partial}{\partial t} f(x, v, t)|_c \quad (1)$$

According to the presentation of Eliasson and Kogelschatz [4] regarding the Boltzmann equation, a the acceleration term, $a = (cE)/m$ (c: electron charge; m: mass of electron), which is proportional to the force from the electric field (E) acting upon the electron. The term on the right-hand side of the equation, $(\partial/\partial t) f(x, v, t)|_c$, is the collision term. It accounts for the electron energy distribution change

due to collisions between electrons and gas species present in the reaction zone [4]. Therefore, this program can determine the energy deposition directed toward the various collision processes: elastic, inelastic, ionization, and attachment. Since the DBD system has a steady-state, uniform electric field at high pressure (1 atm or greater), the electron energy distribution becomes simply a function of velocity. Once $f(v)$ is known, the average electron energy (e_{avg}) can be found for a given reduced electric field, as shown in the following equation [7]:

$$e_{\text{avg}} = \int_0^\infty e(v) f(v)\, \mathrm{d}v, \quad e(v) = \frac{1}{2} m v^2 \tag{2}$$

In addition, since the electron energies within the system are affected by the electric field strength and interactions with gas species present, the average electron energy can be described as a function of the reduced electric field (E/P), which is the electric field divided by the system pressure (P), at the condition of breakdown. Changes that increase the reduced electric field result in an increase in the average electron energy. The reduced electric field is also related to the breakdown strength and is a function of breakdown voltage (V), gas gap distance (D), and system pressure ($E = V/D$ and, therefore, $E/P = V/DP$). Increasing the system pressure or gas gap distance will result in a decrease in the reduced electric field and, hence, the average electron energy within the system [4].

This method, which has been described in detail earlier [8–11], uses a DBD reactor to directly partially oxidize methane to organic oxygenates, such as methanol. Results have shown that a 3:1 methane–oxygen feed has a greater methane conversion rate than a pure methane feed (all other experimental parameters are held constant) [9]. In addition, organic oxygenate products were formed only when oxygen was present in the feed. Here the effect that the partial pressure of oxygen has on methane reaction rate, energy efficiency, and product selectivity for a methane–oxygen system is discussed.

The effects reduced the electric field and, therefore, the average electron energy has on product selectivities are discussed. Also, residence time experiments that help to explain the sequential and parallel product formation pathways that are occurring within the methane–oxygen system are discussed.

Finally, the effect of varying reactor wall temperature allowing increases in organic oxygenate production, while decreasing CO_x production in the partial oxidation of methane are presented.

2. Experimental

Methane and oxygen are fed to the DBD reactor, shown in Fig. 1, by mass flow controllers (Porter Instrument). The methane–oxygen feed enters through the top of the reactor and flows down axially in a gas gap between two concentric cylinders. The inner cylinder is made of glass and acts as the dielectric. This glass dielectric cylinder has a stainless steel metal foil on its inner wall, that acts as an electrode. The outer cylinder is also made of stainless steel and its inner wall acts as the other electrode. Thus, the DBD reactor has a capacitive nature with a glass dielectric that evenly distributes the “micro-discharges” and limits their duration [12]. The reactor is cooled by a water jacket that surrounds the outer reactor shell.

The product stream exits from the bottom of the reactor and flows to a liquid trap cooled by dry ice and acetone (−55°C). Organic oxygenates (principally methanol, formaldehyde, methyl formate, and formic acid) and water are collected in the trap. Some of these products can potentially condense within the reactor due to the low system temperature, and are carried out by the gas stream. The remaining effluent gas stream exits the liquid trap and flows to a Carle 400 AGC with a hydrogen analysis system. The liquid product that was collected from the liquid trap is analyzed with a Varian 3300 GC on a Porapak Q column.

The DBD reactor receives its AC power from an Elgar model 501 SL power supply. The voltage range for the Elgar is from 0 to 130 V, its current range is from 0 to 5.8 A, and its frequency range is from 45 to 5000 Hz. It has a maximum power output of 500 W. A CBK precision generator allows the Elgar power system to produce a sinusoidal waveform at a desired frequency. A 15060 P Franceformer transformer steps up the voltage and applies it to the DBD reactor. The breakdown voltage for the annular reactor is measured using a Tektronix P6015A high voltage probe in conjunction with a Tektronix TDS 754C digital oscilloscope.

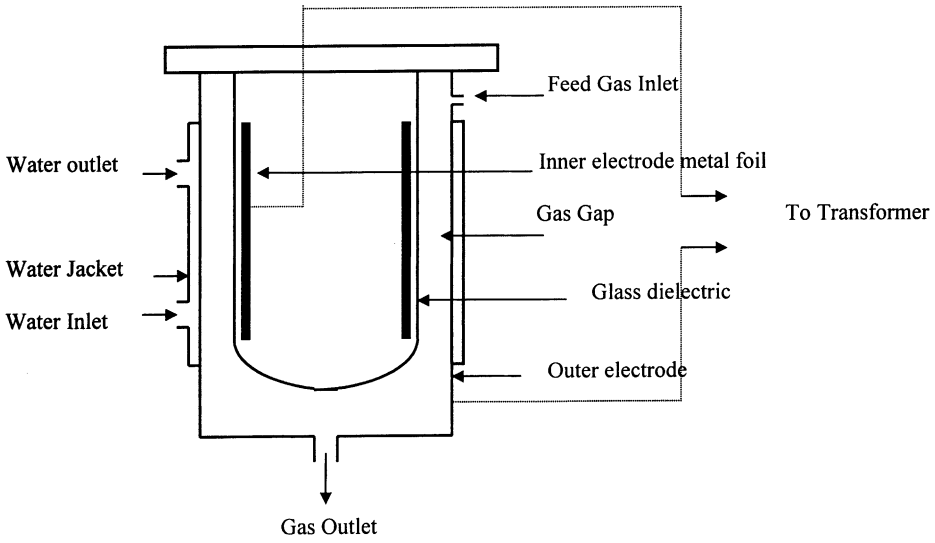

Fig. 1. Annular reactor.

The power is measured with a Microvip 1.2 energy analyzer on the primary side. This allows the system's energy consumption on a per molecule of methane converted basis to be determined (the energy consumption as used in this work is eV per molecule of methane converted and 1 eV per molecule of CH_4 converted = 96.4 kJ/mol = 1.67×10^{-3} kW h/g). As a result of measuring the power on the primary side, the energy losses from the DBD reactor, high voltage wires, and transformer are all included in the measured value. The components (DBD reactor, high voltage wires, and transformer) have not been optimized to minimize these energy losses and, therefore, the real energy efficiency of this process is underestimated.

For the first series of experiments the methane–oxygen feed ratio was varied from 5:1 to 2:1 at 1 atm with a gap distance of 4.0 mm, an electrode reaction area of 688 cm^2, and a residence time of 29 s. The frequency was 173 Hz at 1 atm and the water temperature within the water jacket was 15°C. The power input was 118 W.

The second series of experiments varied the gas gap distance from 1.9 to 12.0 mm in order to determine how changes in the reduced electric field strength affected the results of a 2:1 methane–oxygen system. The residence time for these experiments was 1 min and the reaction area was 688 cm^2. When changing from a gap distance of 1.9–12.0 mm, the frequency was increased from 174 to 216 Hz in order to maintain the power factor at a value of 1, due to the fact that the capacitance of the system changes when the gas gap is altered. The power input was 118 W and the water temperature within the water jacket was 15°C.

The third series of experiments varied the residence time from 2.5 to 40 s in order to better determine the carbon pathways occurring within the system. The reaction area for these experiments was 430 cm^2, the frequency was 198 Hz, and the power input was 118 W. The water temperature within the water jacket was 12°C.

The last series of experiments examined the effect of in situ product condensation on product selectivities. Methane and oxygen are fed to the reactor at a ratio of 3:1 with a total flow rate of 200 cc/min. This gives a residence time of 1 min. The frequency and voltage are set at 100 Hz and 7.6 kV, respectively. The experimental variable for the four experiments conducted is the water-jacket temperature.

Finally, Bolsig, the numerical electron Boltzmann solver by Kinema Software and CPAT, was used to plot all the energy deposition graphs (energy deposition directed toward a given collision process as a function of reduced electric field strength). In addition, it was used to determine the average electron energy within

methane–oxygen systems for a given reduced electric field strengths [5,13].

3. Results and discussion

3.1. Oxygen activation

It has been shown that when going from a pure methane feed to a 3:1 methane–oxygen feed, the methane reaction rate is enhanced due to active oxygen species. In addition, organic oxygenate products are formed only when oxygen is present [9]. This work varies the methane–oxygen feed ratio from 5:1 to 2:1 at 1 atm in order to illustrate the effect of the partial pressure of oxygen on the methane reaction rate, the system's energy consumption per methane converted, and product selectivities. Table 1 shows that increasing the oxygen partial pressure decreases the system's energy consumption per methane converted, when going from 5:1 to 2:1 methane–oxygen system. This is because the methane conversion increased enough to compensate for the 20% decrease in methane partial pressure and throughput. The methane reaction rate, therefore, increased with increasing partial pressure of oxygen in the feed, which caused the decrease in energy consumption per methane converted.

Table 2 shows the product-selectivity results for the methane–oxygen feed ratio experiments. The results show that when going from 5:1 to 2:1 methane–oxygen feed ratio, the CO_x, C_2, and organic oxygenate selectivities remain relatively constant. Previous work as well as the residence time experiments discussed later in this work provide evidence that there is a pathway for partial oxidation of methane directly to CO and/or CO_2 in the DBD methane–oxygen system [11]. With this in mind, the CO_x and organic oxygenate selectivities remain relatively constant when the partial pressure of oxygen is increased in the feed because both pathways are enhanced. The net effect is that changes in the rates of these two oxidative pathways balance out one another. In addition, the ethane selectivity always remains low because, enough atomic oxygen is present to inhibit significant amounts of methane coupling.

3.2. Selectivity control

The next series of experiments varies in the gas gap from 1.9 to 12.0 mm in a 2:1 methane–oxygen system. As previously mentioned, altering the gas gap affects the reduced electric field of a DBD system, which ultimately controls the product distribution. This is analogous to a system controlling the product selectivity through the use of a catalyst. Therefore to begin with, Table 3 shows how the electrical and discharge properties change when the gas gap is varied from 1.9 to 12.0 mm. Increasing the gas gap distance decreases the reduced electric field strength (*E*/*P*), and this results in a decrease in the average electron energy of the plasma. Decreasing the reaction zone's average electron energy in turn affects the energy deposition directed toward the various types of collision processes. Fig. 2 shows the energy deposition for the significant collision processes as a function of reduced electric field strength (*E*/*P*) in a barrier discharge reactor for a 2:1 methane–oxygen system. The experimental operating region for this study lies within the gray region seen in this figure. Within this operating region, at least 97% of the energy being put into the reaction zone is directed toward inelastic methane and oxygen collision processes. Processes such as attachment ($e + A_2 \rightarrow A_2^-$), ionization ($e + A_2 \rightarrow A_2^+ + 2e$), and elastic ($e + A_2 \rightarrow e + A_2$) collision processes are not significant in this range.

Table 1
CH_4:O_2 ratio experimental results[a]

CH_4:O_2	*E*/*P* (V/cm/Torr)	% CH_4 conv.	% O_2 conv.	eV per molecule of CH_4 conv.	Moles of CH_4 conv. (mol/min)
5:1	30	6	31	61	0.0012
4:1	30	6	27	60	0.0012
3:1	30	7	23	58	0.0013
2:1	30	9	22	48	0.0015

[a] 4 mm gas gap, 118 W power input, water-jacket temperature = 15°C, 1 atm.

Table 2
CH_4:O_2 ratio experimental results[a]

CH_4:O_2	% H_2 select.	% CO select.	% CO_2 select.	% Ethane select.	% Ethylene select.	% Acetylene select.	% M select.	% F select.	% MF select.	% FA select.	C_2 sum	Org. oxy. Liquid sum	Sum
5:1	12	16	10	4	0	0	19	12	8	13	4	51	81
4:1	11	16	10	4	0	0	19	15	10	15	4	59	89
3:1	9	15	10	2	0	0	16	15	7	16	2	53	80
2:1	8	16	13	1	0	0	15	14	10	20	1	59	89

[a] 4 mm gas gap, 118 W power input, water-jacket temperature = 15°C, 1 atm. M: methanol; F: formaldehyde; MF: methyl formate; FA: formic acid; selectivity for carbon compounds is on a carbon mole basis; sum: sum of carbon selectivity (mole basis).

Table 3
Electrical parameters and acetylene:ethylene:ethane ratio for gap distance experiments[a]

	Gap distance (mm)			
	1.9	4.0	6.7	12.0
E/P (V/cm/Torr)	49.0	30.0	24.0	18.0
Average electron energy (eV)	5.0	4.2	4.0	3.6
Acetylene:ethylene:ethane	0:0:1	1:0:2	1:0:2	10:1:7

[a] 2:1 CH_4:O_2 system at 1 atm.

Fig. 3 separates the energy deposition for the inelastic methane collision processes into its two primary components: methane excitation and methane dissociation. The two components have electron collision formation energy ranges of 0.2–0.4 and 9.0–12.0 eV, respectively. The collisions involve electrons colliding with methane molecules. The figure shows that, within the experimental operating region, when the reduced electric field is decreased, the energy deposition directed toward methane excitation increases, while that towards methane dissociation decreases. When the reduced electric field is decreased, the average electron energies decrease and the fraction of electrons capable of dissociating methane is reduced. This also means the fraction of electrons capable of exciting, but not dissociating, methane molecules increases and the energy fraction deposited into the excitation process increases.

Fig. 4 separates the energy deposition for the inelastic oxygen collision processes into its two components: oxygen excitation and oxygen dissociation. The two components have electron collision formation energy ranges of 0.2–4.0 and 6.0–8.4 eV, respectively. The collisions involve electrons colliding with oxygen molecules. Within the experimental operating region seen in this figure, a decrease in the reduced electric field strength results in an increase in the energy deposition directed toward the excitation of the oxygen molecules without dissociation. In this same range, the energy deposition directed toward oxygen dissociation remains around 40% for reduced electric field values above 30 V/cm/Torr and drops off significantly below this value. This drop-off occurs because the average electron energy decreases to the point that there is a significant reduction in the fraction of electrons having enough energy to dissociate oxygen molecules and an increasing portion of the electrons will only

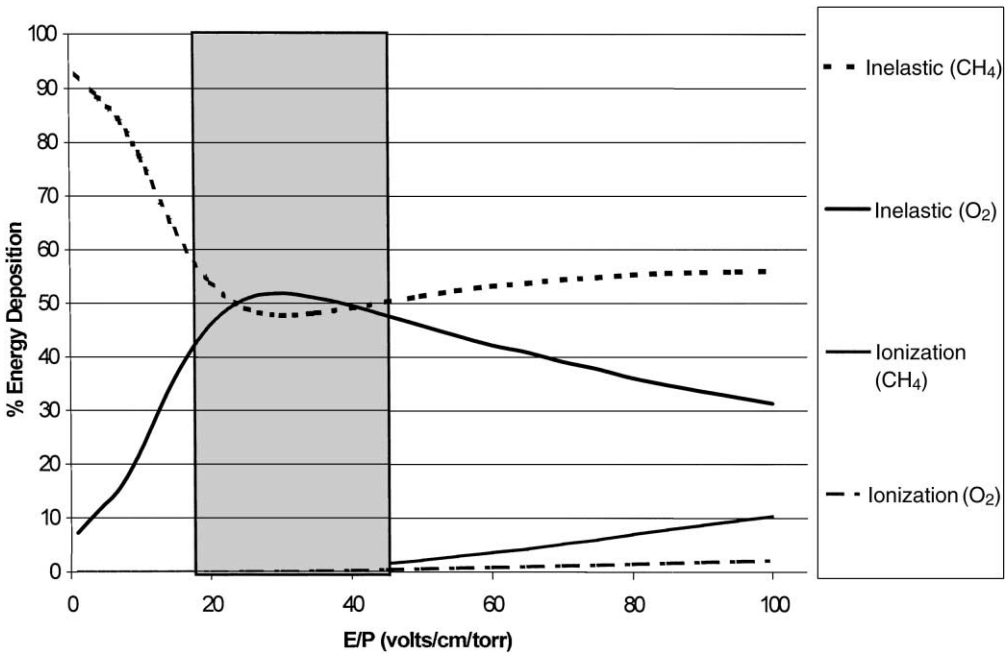

Fig. 2. Energy inputted into collision processes vs. *E/P* (2:1 CH_4:O_2 system).

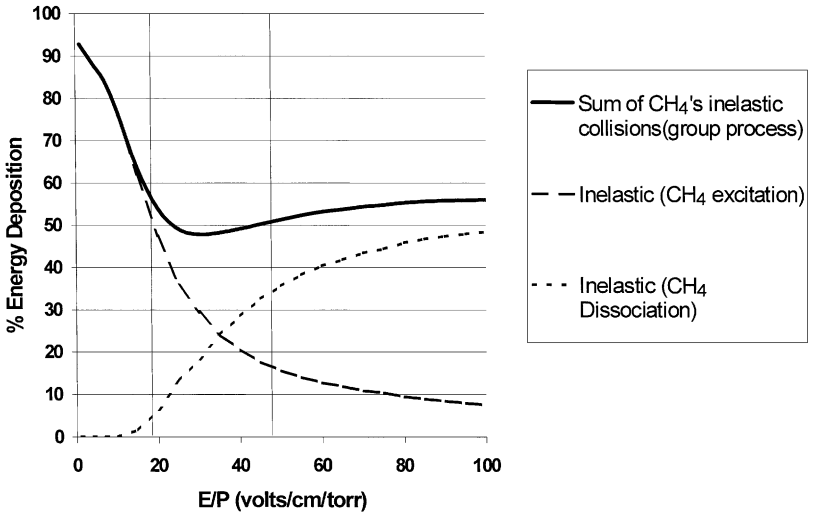

Fig. 3. Energy inputted into CH_4 inelastic collision processes vs. *E*/*P* (2:1 CH_4:O_2 system).

have enough energy to excite oxygen (and methane) molecules.

In addition to the inelastic oxygen collision processes, Fig. 4 also shows the organic oxygenate product selectivity (organic oxygenate product selectivity is equal to the sum of organic oxygenate selectivities) as a function of reduced electric field. The results show that when going from 48 to 30 V/cm/Torr, the organic oxygenate selectivity and the energy deposition going into oxygen dissociation stay relatively constant. However, from 30 to 18 V/cm/Torr, the organic oxygenate product selectivity and the energy deposition going into oxygen dissociation both sharply decrease. Finally, the energy deposition going

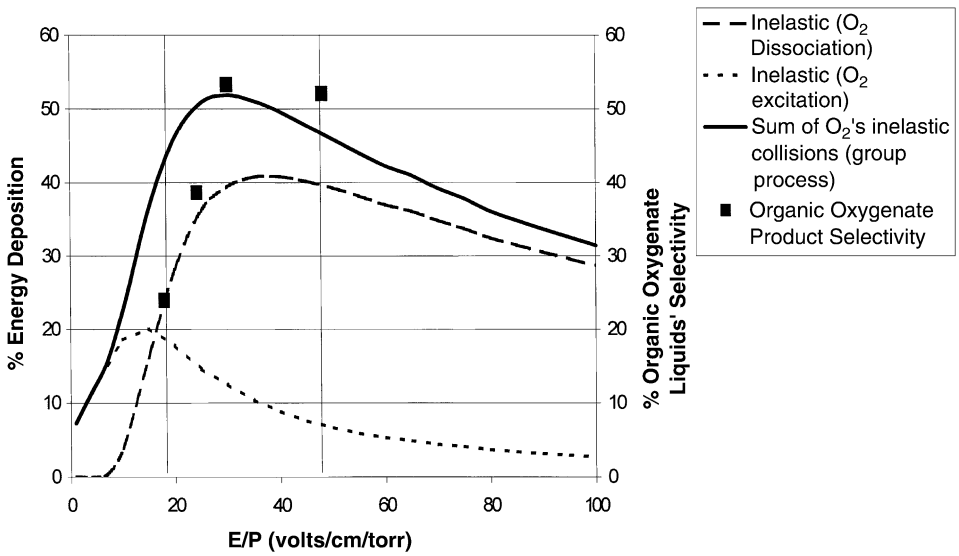

Fig. 4. Energy inputted into O_2 inelastic collision processes and organic oxygenate product selectivity vs. *E*/*P* (2:1 CH_4:O_2 system, 118 W power input, 15°C water-jacket temperature).

into oxygen excitation without dissociation does not follow the organic oxygenate product selectivity trend, since it increases over the entire operating range, from 48 to 18 V/cm/Torr. These results suggest that an atomic oxygen species generated from oxygen dissociation is responsible for the direct partial oxidation of methane to organic oxygenate species.

Fig. 5 shows the gap distance experiments for C_2 hydrocarbon selectivity (sum of acetylene, ethylene, and ethane), the energy deposition directed toward the inelastic methane collision processes and its two components, and the two components for the inelastic oxygen collision processes, as functions of reduced electric field. Table 3 shows the acetylene–ethylene–ethane ratio at a given reduced electric field for these experiments. The results show that when the energy deposition directed toward oxygen dissociation drops off and the energy deposition directed toward the inelastic methane collision process increases (the latter due to the increase in the energy deposition directed toward methane excitation), the C_2 hydrocarbon selectivity increases. The increased C_2 hydrocarbon selectivity is due to increases in ethane and acetylene production. Caldwell [14] has shown in a pure methane system that, when varying the gas gap and, therefore, the reduced electric field over the same range, the product distribution is composed of ethane and hydrogen with some higher alkanes, but no ethylene or acetylene, and is relatively constant. Those pure methane results suggest that ethane formation in the 2:1 methane–oxygen system at the lower reduced electric field strengths (where oxygen dissociation is not significant) comes from methane coupling from direct methane activation, as shown in Fig. 6. In this range of reduced electric field, oxygen dissociation and its consumption of methane is not significant. Also in this same range, with oxygen, increased oxygen excitation occurs (O_2*) with significant acetylene selectivity. This suggests (O_2*) involvement in the production of acetylene, as shown in Fig. 6. Additional evidence that active molecular oxygen species are involved in C_2 hydrocarbon formation comes from the fact that methane conversion rates for the pure methane experiments [14] are less than the methane conversion rates in this study. Further, acetylene production becomes negligible at higher reduced electric field strengths, in which the energy deposition directed

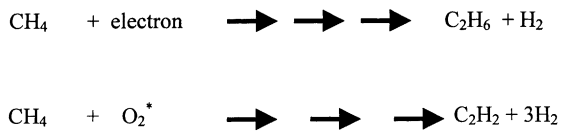

Fig. 6. Hydrocarbon formation pathways for C_2 hydrocarbons at low reduced electric fields ($E/P < 30$ V/cm/Torr).

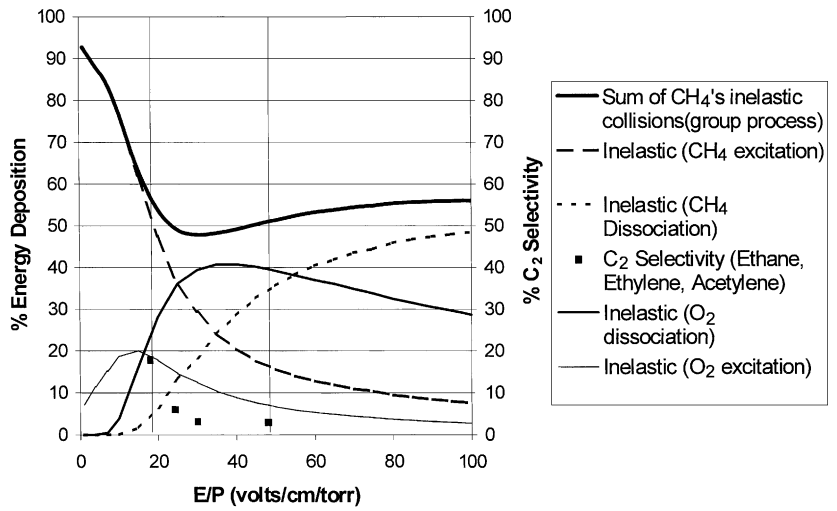

Fig. 5. Energy inputted into CH_4 and O_2 inelastic collision processes and C_2 selectivity vs. E/P (2:1 CH_4:O_2 system, 118 W power input, 15°C water-jacket temperature).

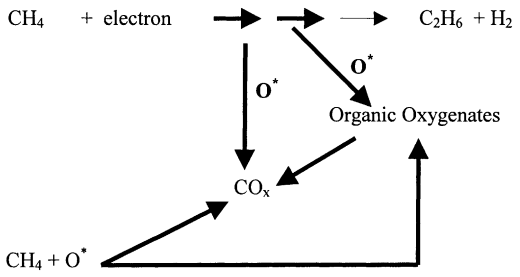

Note: This figure includes CH_4 activation that occurs in Figure 6

Fig. 7. Hydrocarbon formation pathways at high reduced electric fields ($E/P > 30\,V/cm/Torr$) (note: this figure includes CH_4 activation that occurs in Fig. 6).

toward oxygen excitation (O_2^*) is significantly less than that of oxygen dissociation (O^*). Pathways involving the atomic oxygen (O^*) at higher reduced electric field strengths are shown in Fig. 7.

For all reduced electric field strengths, little to no ethylene is observed and this may suggest that acetylene may be formed, as shown in Fig. 6, from the coupling of two CH group species as opposed to ethane reacting sequentially to form ethylene and then acetylene, since the reactions' thermodynamics suggests that this is unlikely to preferentially not favor ethylene. Evidence for the presence of CH groups in low temperature plasmas has been shown by Okumoto and coworkers [15], in which CH groups were detected spectroscopically in a methane–oxygen system using a pulsed DBD reactor. In addition, Caldwell [14] has shown in a DBD reactor that increasing the partial pressure of hydrogen in an ethane–hydrogen system inhibits the production of ethylene and acetylene. In contrast, these results show that acetylene selectivity increases when hydrogen selectivity increases, and this also suggests a different pathway other than sequential dehydrogenation.

The reduced electric field may also be altered by changing the pressure instead of the gap. Results at 2 atm and 4.0 mm gap gives a reduced electric field of 23 V/cm/Torr, giving a variation in the same range of the gap distance experiments.

The organic oxygenate pathways that occur once atomic oxygen initiates the process can be followed by varying the residence time for a 3:1 methane–oxygen system at 1 atm. As the residence time is increased from 2.5 to 40 s, both the methane and oxygen conversions increase 89%. The increase for both methane and oxygen conversions were linear over this range, but previous work has shown that at greater methane and oxygen conversions, the methane and oxygen conversions become non-linear and, therefore, methane and oxygen concentrations do affect the methane reaction rate [11].

Fig. 8 shows the residence time experiment results for the organic oxygenate selectivities. The figure shows that when the residence time increases from 2.5 to 40 s, the methanol selectivity initially decreases rapidly and then decreases more gradually over time. The formic acid selectivity initially increases rapidly, then at a lower rate. Formaldehyde and methyl formate selectivities increase at a uniform rate. This indicates that methane and oxygen react to form methanol as an initial product, which further reacts to form formic acid and formaldehyde. Significant amounts of formic acid are evidently formed from methanol at relatively short residence times and can then react with methanol to form methyl formate. Finally, the organic oxygenate selectivities at 40 s residence time represent the typical selectivities seen with longer residence time experiments (residence time $\geq$ 40 s).

3.3. In situ separation

A significant benefit of lowering the operating temperature, well below that of many heterogeneous catalysis, is the possibility of in situ separations using polymer membranes or product condensation. This is done to assist control of selectivity in a manner that a catalyst might.

The results obtained for partial oxidation experimental series when the reactor wall temperature is varied is shown in Table 4. The results show that changes in water-jacket temperature from 6 to 75°C results in only small changes in methane conversion, while oxygen conversion increased significantly from 67 to 88%. The ethane selectivity remains relatively constant with increasing temperature but the CO and CO_2 selectivities both increase. The "liquid" selectivities, except for methyl formate and ethanol, which shows little change, generally decrease with increasing temperature. Thus, as can be seen in the last two columns of Table 4, the overall trend for increasing water-jacket temperature is that the sum of the liquid

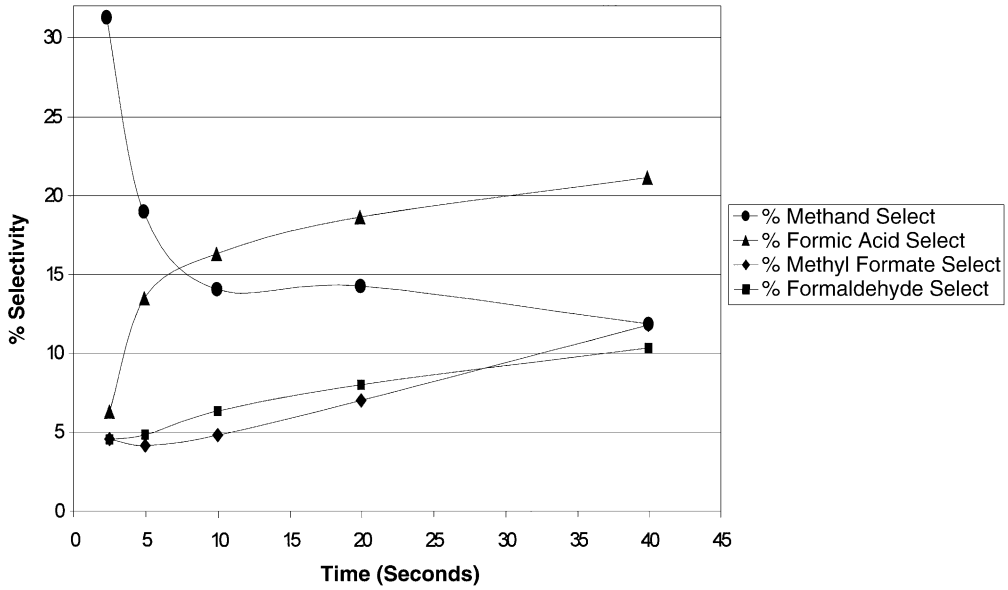

Fig. 8. Organic oxygenate selection vs. residence time.

Table 4
Organic oxygenate in situ removal experiments[a]

H_2O temperature (°C)	CH_4 conv. (mol%)	O_2 conv. (mol%)	% C selectivity (mole basis)									
			CO_2	CO	Et	M	MF	FA	F	E	% Org. liquid sum	% Gas phase sum
6	23	67	10	11	3	11	3	15	15	1	45	24
28	24	74	13	14	4	17	5	16	13	1	52	31
54	24	81	22	25	4	9	5	12	7	1	34	51
75	25	88	26	36	3	9	4	7	4	0	24	65

[a] Cylindrical reactor, 3:1 CH_4:O_2, 7.6 kV, 100 Hz, 200 cc/min flow rate. M: methanol; MF: methyl formate; FA: formic acid; F: formaldehyde; E: ethanol; Et: ethane.

selectivities decreases, while the sum of the "gas" selectivities increase. The increased selectivities for CO_x at higher temperatures due to "over" oxidation of the liquid products is consistent with higher oxygen conversion with little change in methane conversion. Because the reactor operates at such low temperatures, as the methane conversion increases as the gases pass along the length of the reactor, the partial pressures of the products increase. The partial pressures of the heavier liquid components reach their vapor pressures at sufficiently low temperatures that condensation on the cooled wall occurs. Thus, under ideal conditions, the low temperatures achievable in these reactors result in low partial pressures of these products in the gas phase, thus minimizing their availability to be further oxidized to gas products CO_x.

4. Conclusions

The product selectivities in a methane–oxygen system within a DBD system can be affected by altering the reduced electric field strength by changing the geometry or operating conditions. These changes affect the average electron energy within the system and can shift the energy deposition among the

various collision processes. This was shown in a 2:1 methane–oxygen system through the shift in product selectivities from organic oxygenate products to C_2S when the reduced electric field strength went from 30 to 18 V/cm/Torr by increasing the gap distance from 4.0 to 12.0 mm. Residence time studies showed that methane partially oxidizes to form methanol, which further reacts to form formic acid, formaldehyde, and methyl formate. These results also support the conclusion that there is a direct oxidative route from methane to CO and/or CO_2 since there is a significant amount of both of them present at even low residence times, and this is consistent with previous work [11]. All of the results are consistent with the changes of the populations of active species with changes in energy deposition due to changes in the reduced electric field. In the range studied, a lower reduced electric field reduces oxygen dissociation and increases methane and oxygen excitations. Lower oxygen dissociation reduces organic oxygenates, but higher methane and oxygen excitations decreases energy consumption per molecule of methane converted.

In addition, the results of this study show that product selectivities are strongly influenced by in situ product condensation in partial oxidation of methane in a DBD reactor when reactor wall temperature is varied. At 28°C, 52% of the reacted carbon is recovered as these liquid organic oxygenates. At 75°C, only 24% of the reacted carbon is recovered as liquid organic products. When the temperature of the system is lowered sufficiently the vapor pressures of the liquid organic oxygenates are reduced and condensation can occur, thus limiting the partial pressures of these desirable products in the gas phase. This results in reduced oxidation of these products to CO_x.

Acknowledgements

The support of Texaco, Inc., the United States Department of Energy under Contract DE-FG21-94MC31170, and the National Science Foundation for a Graduate Traineeship are gratefully acknowledged.

References

[1] R.J. Farrauto, C.H. Bartholomew, Fundamentals of Industrial Catalytic Processes, Blackie, London, 1997.
[2] M.T. Wolfe, Catalyst Handbook, 2nd Edition, 1989.
[3] G. Barbieri, P. Di Maio, Francesco, Simulation of the methane steam re-forming process in a catalytic Pd-membrane reactor, Ind. Eng. Chem. Res. 36 (1997) 2121–2127.
[4] B. Eliasson, U. Kogelschatz, Nonequilibrium volume plasma chemical processing, IEEE Trans. Plasma Sci. 19 (6) (1991).
[5] Bolsig, CPAT and Kinema Software, 1998. http://www.csn.net/siglo/bolsig.htm.
[6] L.C. Pitchford, S.V. Oneil, J.R. Rumble, Extended Boltzmann analysis of electron swarm parameters, Phys. Rev. A 23 (1) (1980).
[7] L.-M. Zhou, Non-thermal plasma features in dielectric barrier discharges, Written Report, Institute for Gas Utilization Technologies, University of Oklahoma, November 1998.
[8] R. Bhatnagar, R.G. Mallinson, Methane conversion in AC electric discharges at ambient conditions, Methane and Alkane Conversion Chemistry, Plenum Press, New York, 1995, pp. 249–264.
[9] D.W. Larkin, T.A. Caldwell, L.L. Lobban, R.G. Mallinson, Oxygen pathways and carbon dioxide utilization in methane partial oxidation in ambient temperature electric discharges, Energy Fuels 12 (4) (1998) 740–744.
[10] D.W. Larkin, S. Leethochawalit, T.A. Caldwell, L.L. Lobban, R.G. Mallinson, Carbon pathways, CO_2 utilization, and in situ product removal in low temperature plasma methane conversion to methanol, Greenhouse Gas Control Technologies, Elsevier, Amsterdam, 1999, pp. 397–402.
[11] D.W. Larkin, L.L. Lobban, R.G. Mallinson, Production of organic oxygenates in the partial oxidation of methane in a silent electric discharge reactor, Ind. Eng. Chem. Res., Web Release Date: February 28, 2001.
[12] B. Eliasson, W. Elgi, U. Kogelschatz, Modeling of dielectric barrier discharge chemistry, Pure Appl. Chem. 66 (6) (1994) 1275–1286.
[13] The Siglo Data Base, CPAT and Kinema Software, 1998. http://www.csn.net/siglo.
[14] T.A. Caldwell, Personal communication.
[15] A. Mizuno, S. Katsura, M. Okumoto, Direct synthesis of methanol using non-thermal plasma, Reports of Project Research No. 256, Ministry of Education of Japan, 1998, pp. 21–27.